Small-q phonon-mediated unconventional superconductivity in the iron pnictides

A. Aperis,[1,*] P. Kotetes,[1,2] G. Varelogiannis,[1] and P. M. Oppeneer[3]
[1]*Department of Physics, National Technical University of Athens, GR-15780 Athens, Greece*
[2]*Institut für Theoretische Festkörperphysik, Karlsruhe Institute of Technology, D-76128 Karlsruhe, Germany*
[3]*Department of Physics and Materials Science, Uppsala University, Box 530, S-751 21 Uppsala, Sweden*
(Received 9 December 2010; published 22 March 2011)

We report self-consistent calculations of the gap symmetry for iron-based high-temperature superconductors using realistic small-q phonon-mediated pairing potentials and four-band energy dispersions. When both electron and hole Fermi surface pockets are present, we obtain the nodeless $s_\pm$ state that was first encountered in a spin-fluctuation mechanism picture. Nodal $s_\pm$ as well as other gap structures such as $d_{x^2-y^2}$, $s_\pm + d_{x^2-y^2}$, and even a p-wave *triplet* state, are accessible upon doping within our phononic mechanism. Our results *resolve* the conflict between phase-sensitive experiments reporting a gap changing sign, attributed previously only to a nonphononic mechanism, and isotope effect measurements proving the involvement of phonons in the pairing.

DOI: 10.1103/PhysRevB.83.092505 PACS number(s): 74.70.Xa, 71.27.+a, 74.20.−z

One of the foremost issues in contemporary condensed-matter physics is the nature of the medium-high-temperature superconductivity (SC) in the recently discovered iron pnictides.[1] The focal point of current research is to understand whether the bosonic pairing that drives the SC is due to spin fluctuations or phonons and how the pairing mechanism concurs with the emerging symmetry of the superconducting gap.[2] Experimental techniques have recently given controversial results.[3,4] Angular-resolved photoemission spectroscopy and Andreev spectroscopy indicate one nearly isotropic gap or two isotropic gaps,[5–7] whereas penetration depth[8,9] and nuclear magnetic resonance (NMR)[10,11] measurements support both nodeless and nodal gap structures. Moreover, very recent experiments on the evolution of the SC gap symmetry of $LaFeAsO_{1-x}F_x$ with doping conclude that there is a transition from nodeless to nodal SC upon moving from the underdoped to the overdoped regime of this compound.[12] Notably, a nodeless gap is not necessarily a conventional isotropic s-wave gap here.

An important ingredient for discussing the gap symmetry is the Fermi surface (FS) of both 1111 (LaOFeAs) and 122 ($BaFe_2As_2$) parent compounds, which is remarkably simple. The strongly two-dimensional FS mainly consists of two electron and two hole pockets, with a nesting wave vector $\mathbf{Q} = (\pi,\pi)$ connecting them in the folded Brillouin zone (BZ).[13,14] FS nesting stabilizes a spin density wave that yields to SC upon doping.[15] If spin fluctuations mediate the pairing, then a nodeless unconventional superconducting gap reversing its sign between the electron and the hole FS sheets is expected, and is known as the $s_\pm$ state.[2,14,16,17]

Phase-sensitive experiments are needed to distinguish the $s_\pm$ state from the conventional isotropic s-wave state, and indeed, inelastic neutron scattering results appear to be compatible with the coherence factors of the $s_\pm$ state.[3] This has been interpreted as evidence of a nonphononic pairing mechanism probably involving spin fluctuations. However, a systematic NMR study of the dependence of low-lying excitations on fluorine doping in $LaFeAsO_{1-x}F_x$ has shown that antiferromagnetic (AFM) fluctuations are suppressed with doping, while T_c remains unaffected, implying that AFM fluctuations may be irrelevant to SC.[18] Most importantly, isotope effect measurements[4] directly prove the involvement of the phonons in the pairing mechanism. Additional experimental findings do support the relevance of phonons in the pairing.[19] However, how this could be compatible with a gap that changes sign is mysterious.

In this report we propose a new picture for SC in the iron pnictides on the basis of self-consistent calculations of the gap symmetry. First, we argue that small-q electron-phonon scattering dominates the pairing. Second, we show that this solely phononic mechanism in the presence of strong Coulombic interactions can naturally produce the unconventional gap symmetries proposed for the pnictides. When both electron and hole FS pockets are present, the nodeless $s_\pm$ gap is obtained self-consistently, because of the intricate four-band pnictide FS combined with strong interband scattering. Third, nodal gap structures may also develop when going from underdoped to overdoped regimes upon doping. These include $s_\pm$, $d_{x^2-y^2}$-wave, $s_\pm + d_{x^2-y^2}$, and even p-wave triplet SC.

The effective electron-phonon interaction may be dominated by the forward processes only when the Coulomb interaction is short range or Hubbard-like,[20,21] which is a requirement for antiferromagnetism as well. Therefore, the proximity of the AFM and small-q phonon mediated SC phases is natural, and this is indeed the case in the pnictides. Unconventional SC due to small-q phonon pairing has already been considered for high-T_c cuprate,[21–23] heavy fermion,[24] organic,[25] and cobaltite[26] systems.

Our aim is to describe the electronic structure of the iron pnictides around the Fermi energy as realistic as possible. To this end we construct a four-band tight-binding model that captures the essential physics of the undoped compounds, while combining features from the previously introduced tight-binding models.[27] The energy bands are

$$\begin{aligned}\epsilon^h_{1,2} &= -t_1^{h_{1,2}}(\cos k_x + \cos k_y) - t_2^h \cos k_x \cos k_y - \epsilon_F^{h_{1,2}},\\ \epsilon^e_{1,2} &= -t_1^e(\cos k_x + \cos k_y) - t_2^e \cos k_x \cos k_y - \epsilon_F^e\\ &\quad \pm t_3^e \sin k_x \sin k_y,\end{aligned} \tag{1}$$

with $t_1^e = -1.14$, $t_2^e = -0.2$, $t_3^e = 0.2$, $\epsilon_F^e = -1.5$, $t_1^{h_1} = -0.3$, $t_1^{h_2} = -0.2$, $t_2^h = -0.24$, $\epsilon_F^{h_1} = 0.6$, and $\epsilon_F^{h_2} = 0.4$. We have verified that that these tight-binding dispersions are in good agreement with band structure calculations; not only are the FS topology and the susceptibility reproduced (see Fig. 1),

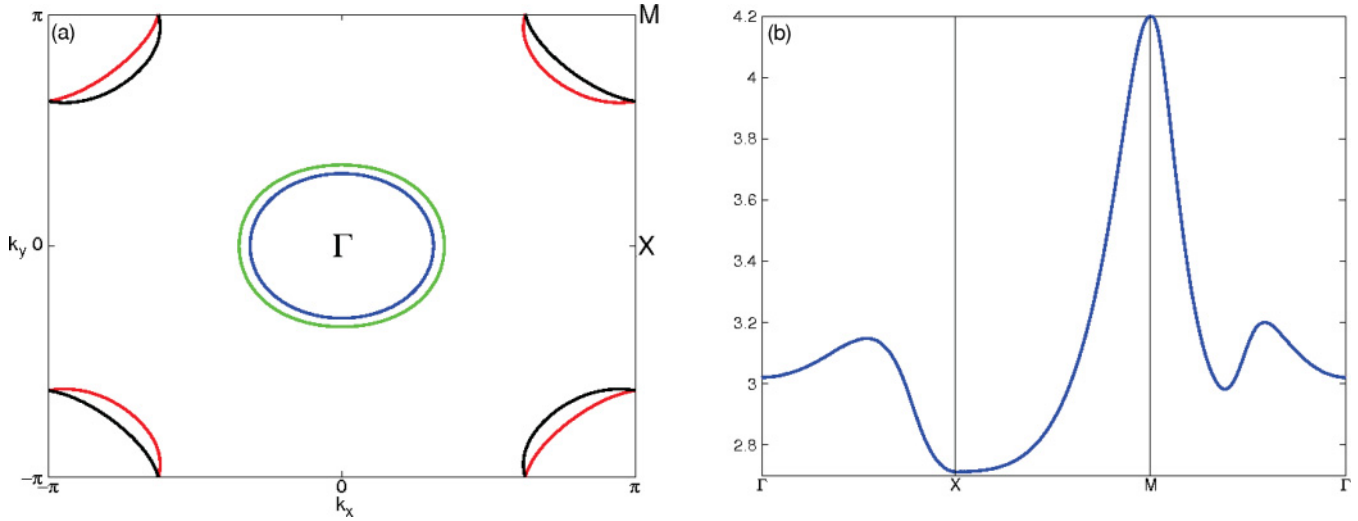

FIG. 1. (Color online) (a) Fermi surface contour of the undoped pnictide compounds in our four-band model. (b) Wave-vector dependence of the static spin susceptibility along high-symmetry lines. The peak indicates well-nested electron-hole pockets at $\boldsymbol{Q} = (\pi,\pi)$.

but also the angularly resolved density of states (arDOS) at any Fermi momentum k_F is given properly [arDOS $\sim |\nabla\epsilon^{e,h}_{1,2}(\mathbf{k}_F)|^{-1}$]. To probe the doping dependence of the gap symmetry in our self-consistent calculations, we have introduced a chemical potential μ varying in the interval $-0.6 \leqslant \mu \leqslant 1.4$. When $\mu > 0$ ($\mu < 0$), the system is electron (hole) doped. The FSs at various chemical potentials as well as the corresponding arDOS are depicted in Fig. 2.

We solve the most general multiband Bardeen-Cooper-Schrieffer (BCS) equation at zero temperature,[28]

$$\Delta_n(\mathbf{k}) = -\sum_{n',\mathbf{k}'} V_{nn'}(\mathbf{k},\mathbf{k}')\frac{\Delta_{n'}(\mathbf{k}')}{2E_{n'}(\mathbf{k}')}, \qquad (2)$$

where $\Delta_n(\mathbf{k})$ is the momentum-dependent superconducting gap, and $E_n(\mathbf{k}) = \sqrt{\epsilon_n^2(\mathbf{k}) + \Delta_n^2(\mathbf{k})}$ the quasiparticle excitation spectrum of the nth band. The pairing potentials $V_{nn'}(\mathbf{k},\mathbf{k}')$ can support intraband ($n = n'$) and interband ($n \neq n'$) scattering. As a first approximation, we take $V_{nn'}(\mathbf{k},\mathbf{k}') = V(\mathbf{k},\mathbf{k}')$. This yields a "global" SC gap symmetry valid over the entire BZ, which is nevertheless driven by the characteristics of each separate band, such as the arDOS distribution.

The effective pairing potential of the small-q phonon-mediated interaction takes the form[23] $V(\mathbf{k},\mathbf{k}') = V_c^* - \frac{V_{\rm ph}}{q_c^2+|\mathbf{k}-\mathbf{k}'|^2}$ properly continued periodically, where a repulsive Coulomb pseudopotential V_c^* is responsible for screening at short distances, whereas the negative term is the attractive phonon part. The pairing kernel is characterized by a smooth momentum cutoff q_c, which selects the small wave vectors in the attractive phonon part, while at larger wave vectors the repulsive Coulomb pseudopotential may prevail. Decreasing the cutoff q_c leads to a situation that has been named *momentum decoupling* (MD).[21] In the MD regime there is a tendency for SC to decorrelate in the various FS regions; the gap function gradually loses its rigidity in momentum space. In regions of the FS with a high arDOS we observe higher gap amplitudes, whereas in low-arDOS regions the gap is smaller. This arDOS-driven anisotropy of the gap is the fingerprint of MD[21] and may be behind multiple gap signatures in the experiments.

To solve the BCS equation self-consistently with the momentum-dependent pairing kernel, we perform the convolution integral in Eq. (2) by utilizing an FFT cyclic convolution technique. The $\mathbf{k}$ summation was performed over a 512×512 grid in a thin shell around the FS, to get maximal resolution. In the results presented here, the Coulomb pseudopotential is fixed at $V_c^* = 0.09V_{\rm ph}$ and the pairing amplitude at $V_{\rm ph} = 2$. Several values of the cutoff parameter q_c were considered, varying from π to $\pi/8$, and various values of the chemical potential were explored.

When $q_c \gtrsim \pi/5$, anisotropic s-wave, sign-preserving solutions are found at all dopings. Further reducing q_c yields interesting doping-induced transitions between different gap symmetries. When $\pi/5 \geqslant q_c > \pi/8$ we get remarkably self-consistent solutions of the gap, depending on the doping level, that include nodal $s_p + d_{x^2-y^2}$-wave, $s_\pm$, $d_{x^2-y^2}$-wave, and p-wave symmetries. Here we present calculations for $q_c = \pi/6$ as a representative example of our results. Figure 2 depicts the evolution of the FS, colored by arDOS^{-1} as a function of doping. In the same plots, the lines where the respective self-consistently calculated SC gap vanishes are drawn.

Starting from the electron doped side, we find an anisotropic $d_{x^2-y^2}$-wave gap in the regime $1.4 \geqslant \mu \geqslant 1.0$ as shown in Fig. 4(a). In this doping region, the high-DOS hole pockets lie away from the Fermi level, and only the electron pockets drive SC. The SC gap contains nodes intersecting the FS in the lowest arDOS points [Fig. 2(a)]. The arDOS distribution at these dopings is highly anisotropic with the points where the gap nodes intersect the FS having the notably lowest DOS. Thus, gapping the rest of the FS while having nodes at the lowest DOS points is energetically favorable for SC.

Decreasing μ shrinks the electron pockets and makes the arDOS more isotropically distributed. When $0.95 \geqslant \mu \geqslant 0.65$, a structure of the p-wave ($\sin k_x$) type develops, with nodes at the locations where the electron pockets cross [Figs. 2 and 4(b)]. Although these FS points have the maximal arDOS, this is only approximately 2 times larger than the minimum arDOS on the FS. The system can still minimize its energy by keeping the rest of the FS gapped while leaving nodes

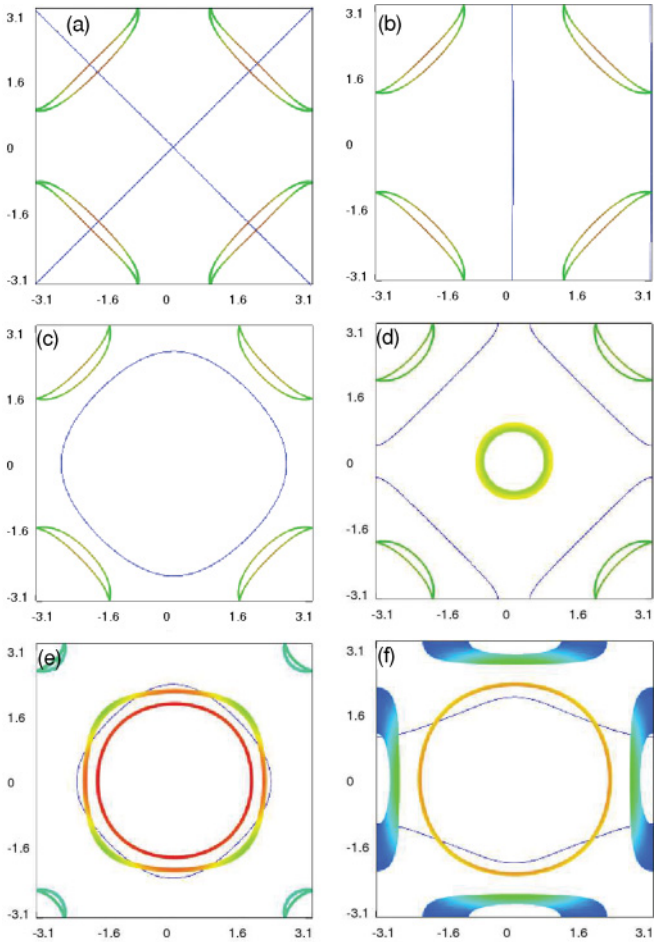

FIG. 2. (Color online) Contours of the FS, in the folded BZ, colored with arDOS^{-1} for (a) $\mu = 1.0$, (b) $\mu = 0.75$, (c) $\mu = 0.45$, (d) $\mu = 0.1$, (e) $\mu = -0.4$, and (f) -0.6. Red FS lines indicate a small arDOS. Blue lines plot the points where the respective, self-consistently obtained, SC gap vanishes ($q_c = \pi/6$). Around half-filling we find an $s_\pm$ gap that persists in the electron-doped (d; $\mu = 0.1$) as well as the hole-doped region [see Fig. 4(c)]. The $s_\pm$ gap is *nodeless,* with its vanishing area almost halfway between the electron and the hole pockets and persisting at further electron doping even when the hole bands do not contribute to the FS (c). More electron doping results in a cascade of transitions to *triplet* ($\sin k_x$) (b) and $d_{x^2-y^2}$-wave (a) solutions. For $\mu < 0$, the nodes of the $s_\pm$ solution move closer to the outer hole pocket and, finally, intersect it (e). In the doping limit when the FS becomes as in (f), the SC gap is a superposition of $s_\pm + d_{x^2-y^2}$ symmetries. Note that the hole FS is thicker than the electron FS due to its higher DOS, therefore we chose to use a different color grade for the electron and hole bands.

on these points. Since SC, in our approach, originates from particle pairing in the same band, the symmetry of the gap function implies a *spin-triplet* order parameter. Such a state has already been proposed for iron pnictides in a different context.[29] However, a spin-singlet p-wave order parameter is also possible if one considers interband pairing.[30]

In the interval $0.6 \geqslant \mu \geqslant 0.25$, a nodeless $s_\pm$ gap is found, yet with the nodal lines close to the electron pockets [Fig. 2(c)]. The anisotropy of the arDOS is further reduced and any node on the FS is not the preferred configuration. This $s_\pm$ solution

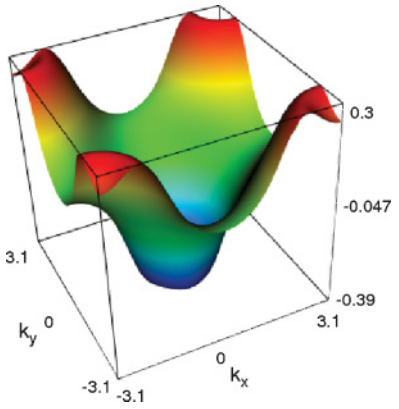

FIG. 3. (Color online) A typical, self-consistently obtained sign changing $s_\pm$ superconducting gap, originating from a small-q phonon interaction. The zeros of this gap emerge between the electron and the hole pockets (for $q_c = \pi/6$ and $\mu = -0.1$). Note the anisotropy of the gap function and how the gap amplitude varies over different regions.

is mainly a superposition of $\cos k_x \cos k_y + (\cos k_x + \cos k_y)$ representations with different weights. As we move toward half filling, the hole pockets approach the Fermi level, the $\cos k_x \cos k_y$ component is suppressed and the nodes of the gap move away from the electron pockets.

Around half-filling, $0.2 \geqslant \mu \geqslant -0.3$, the calculations converge to an SC gap of the form shown in Fig. 2(d), which is of the *nodeless* $s_\pm$ type [cf. Fig. 4(c)]. In this regime, the FS consists of both electron and hole bands and the node lines lie almost halfway between them. This happens due to MD

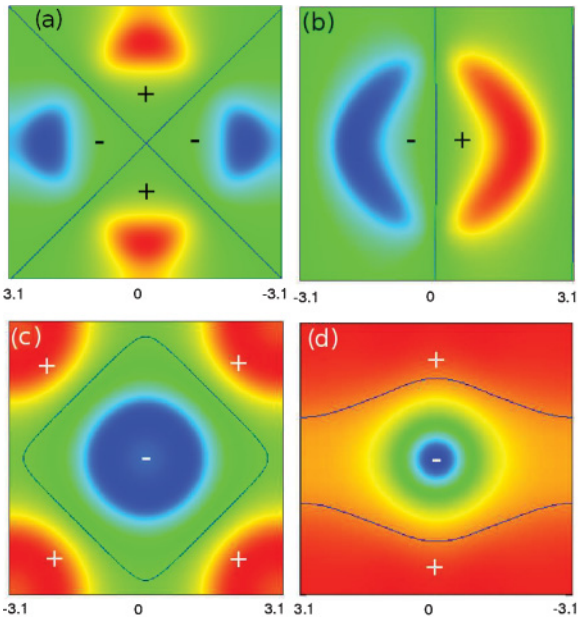

FIG. 4. (Color online) Color-grade plots of characteristic superconducting gap amplitudes in the folded BZ calculated self-consistently, when moving from the electron- to the hole-doped regime for $q_c = \pi/6$. (a) $\mu = 1.15$, (b) $\mu = 0.8$, (c) $\mu = -0.1$, and (d) $\mu = -0.6$, respectively. The corresponding FS shapes are depicted in Fig. 2. Thin blue lines indicate the locations where the obtained SC gap vanishes. In the color grade, red illustrates a positive, and blue a negative, sign of the maximal gap.

phenomena and the presence of interband coupling between the bands. The latter makes the SC gaps over the hole and electron FS coupled, while the former ensures that maximum energy is gained by leaving the empty (no-FS) space between these FS sheets ungapped. This mechanism results in a sign-alternating $s_{\pm}$ solution over the entire BZ. The gap is nearly isotropic or may exhibit some arDOS-driven momentum anisotropy (see Fig. 3) and corresponds to the nearly isotropic BCS-like gap reported in several experiments.[5–7]

Upon further doping the system with holes, $-0.35 \geqslant \mu \geqslant -0.55$, the nodes of the $s_{\pm}$ gap intersect the outer hole FS [Fig. 2(e)]. Finally, at $\mu = -0.6$ the FS and the arDOS distribution become as shown in Fig. 2(f). The gap now is a superposition of $s_{\pm}$ and $d_{x^2-y^2}$ symmetries, with nodes at the low arDOS points of the FS. This rich structure agrees with previous theoretical studies suggesting the near-degeneracy of these two symmetries.[17] Along with the pure $d_{x^2-y^2}$-wave, p-wave, and $s_{\pm}$ solutions, this gap structure offers a possible explanation of the NMR and penetration depth reports of nodal SC in both electron- and hole-doped compounds.[8,10] Note that our theory predicts transitions from nodeless to nodal SC when going from the underdoped to the overdoped regime (with either hole or electron doping). Exactly this behavior was recently found experimentally.[12]

In conclusion, we have self-consistently computed the BCS gap of electron- and hole-doped iron pnictides. Our study offers a scenario for understanding the gap symmetry of the superconducting state in these materials. We have shown that small-q electron-phonon scattering can accommodate conflicting experimental results producing a gap that changes sign while being compatible with the observed isotope effect. When both electron and hole FS sheets are present, we obtain within this purely phononic mechanism, as a self-consistent solution, the fully gapped $s_{\pm}$ state, which was so far considered evidence of a spin-fluctuation mechanism. Depending on doping, the computed gap symmetries vary from nodeless to nodal, in agreement with recent observations. Our solutions include $s_{\pm} + d$-wave in the hole-doped side and d-wave, as well as spin-triplet, gap functions in the electron-doped side. The present results establish that the small-q phonon picture for the pairing mechanism in the iron pnictides can explain the conflicting observations and, hence, is the plausible one. Understanding the competition of SC with spin density waves as well as magnetoelastic effects when forward processes dominate the electron-phonon interaction could provide further insight.

We are grateful to J. G. Analytis for enlightening discussions. A.A. and P.K. acknowledge financial support from the NTU Athens; P.K., from the EU under Project NanoCTM; and P.M.O., from the Swedish Research Council (VR).

*Corresponding author: aaperis@central.ntua.gr

[1] Y. Kamihara *et al.*, J. Am. Chem. Soc. **130**, 3296 (2008).
[2] I. I. Mazin and J. Schmalian, Physica C **469**, 614 (2009), and references therein.
[3] A. D. Christianson *et al.*, Nature **456**, 930 (2008).
[4] R. H. Liu *et al.*, Nature **459**, 64 (2009).
[5] T. Y. Chen *et al.*, Nature **453**, 1224 (2008).
[6] H. Ding *et al.*, Europhys. Lett. **83**, 47001 (2008).
[7] T. Kondo *et al.*, Phys. Rev. Lett. **101**, 147003 (2008).
[8] C. Martin *et al.*, Phys. Rev. Lett. **102**, 247002 (2009).
[9] L. Malone, J. D. Fletcher, A. Serafin, A. Carrington, N. D. Zhigadlo, Z. Bukowski, S. Katrych, and J. Karpinski, Phys. Rev. B **79**, 140501(R) (2009).
[10] H-J. Grafe *et al.*, Phys. Rev. Lett. **101**, 047003 (2008).
[11] M. Yashima *et al.*, J. Phys. Soc. Jpn. **78**, 103702 (2009).
[12] Y. Li *et al.*, New J. Phys. **12**, 083008 (2010).
[13] D. J. Singh and M. H. Du, Phys. Rev. Lett. **100**, 237003 (2008); K. Haule, J. H. Shim, and G. Kotliar, *ibid.* **100**, 226402 (2008); Z. P. Yin, S. Lebegue, M. J. Han, B. P. Neal, S. Y. Savrasov, and S. Y. Pickett, *ibid.* **101**, 047001 (2008); D. J. Singh, Phys. Rev. B **78**, 094511 (2008); C. Cvetkovic and Z. Tesanovic, Europhys. Lett. **85**, 37002 (2009).
[14] I. I. Mazin, D. J. Singh, M. D. Johannes, and M. H. Du, Phys. Rev. Lett. **101**, 057003 (2008).
[15] Clarina de la Cruz *et al.*, Nature **453**, 899 (2008).
[16] K. Kuroki, S. Onari, R. Arita, H. Usui, Y. Tanaka, H. Kontani, and H. Aoki, Phys. Rev. Lett. **101**, 087004 (2008); Z. J. Yao, J. X. Li, and Z. D. Wang, New J. Phys. **11**, 025009 (2009); K. Seo, B. A. Bernevig, and J. Hu, Phys. Rev. Lett. **101**, 206404 (2008); F. Wang, H. Zhai, Y. Ran, A. Vishwanath, and D. H. Lee, *ibid.* **102**, 047005 (2009); R. Sknepnek, G. Samolyuk, Y. B. Lee, and J. Schmalian, Phys. Rev. B **79**, 054511 (2009).
[17] S. Graser *et al.*, New J. Phys. **11**, 025016 (2009); R. Thomale, C. Platt, J. Hu, C. Honerkamp, and B. A. Bernevig, Phys. Rev. B **80**, 180505(R) (2009).
[18] Y. Nakai, S. Kitagawa, K. Ishida, Y. Kamihara, M. Hirano, and H. Hosono, Phys. Rev. B **79**, 212506 (2009).
[19] M. Granath, J. Bielecki, J. Holmlund, and L. Borjesson, Phys. Rev. B **79**, 235103 (2009).
[20] K. J. von Szczepanski and K. W. Becker, Z. Phys. B **89**, 327 (1992); M. L. Kulic and R. Zeyher, Phys. Rev. B **49**, 4395 (1994); A. A. Abrikosov, Physica C **222**, 191 (1994).
[21] G. Varelogiannis, Phys. Rev. B **57**, 13743 (1998).
[22] A. A. Abrikosov, Phys. Rev. B **53**, R8910 (1996); **56**, 446 (1997); A. J. Leggett, Phys. Rev. Lett. **83**, 392 (1999); M. Weger and M. Peter, Physica C **317-318**, 252 (1999).
[23] G. Varelogiannis, A. Perali, E. Cappelluti, and L. Pietronero, Phys. Rev. B **54**, R6877 (1996); G. Varelogiannis, *ibid.* **57**, R732 (1998); A. Perali and G. Varelogiannis, *ibid.* **61**, 3672 (2000).
[24] D. F. Agterberg, V. Barzykin, and L. P. Gorkov, Phys. Rev. B **60**, 14868 (1999); P. M. Oppeneer and G. Varelogiannis, *ibid.* **68**, 214512 (2003).
[25] G. Varelogiannis, Phys. Rev. Lett. **88**, 117005 (2002).
[26] X.-S. Ye, Z.-J. Yao, and J.-X. Li, J. Phys. Condens. Matter **20**, 045227 (2008).
[27] M. M. Korshunov and I. Eremin, Phys. Rev. B **78**, 140509(R) (2008); S. Raghu, X. L. Qi, C. X. Liu, D. J. Scalapino, and S. C. Zhang, *ibid.* **77**, 220503(R) (2008).
[28] H. Suhl, B. T. Matthias, and L. R. Walker, Phys. Rev. Lett. **3**, 552 (1959).
[29] P. A. Lee and X.-G. Wen, Phys. Rev. B **78**, 144517 (2008).
[30] X. Dai, Z. Fang, Y. Zhou, and F. C. Zhang, Phys. Rev. Lett. **101**, 057008 (2008).